

Improving Memory Hierarchy Utilisation for Stencil Computations on Multicore Machines*

Alexandre Sena

Institutos Superiores de Ensino La Salle, Niterói, RJ, Brazil

Aline Nascimento, Cristina Boeres, Vinod E. F. Rebello

{aline,boeres,vinod}@ic.uff.br

Instituto de Computação, Universidade Federal Fluminense (UFF), Brazil

André Bulcão

bulcao@petrobras.com.br

Centro de Pesquisas e Desenvolvimento Leopoldo Américo Miguez de Mello, Petrobras, RJ, Brasil

August 10, 2021

Abstract

Although modern supercomputers are composed of multicore machines, one can find scientists that still execute their legacy applications which were developed to monocore cluster where memory hierarchy is dedicated to a sole core. The main objective of this paper is to propose and evaluate an algorithm that identify an efficient blocksize to be applied on MPI stencil computations on multicore machines. Under the light of an extensive experimental analysis, this work shows the benefits of identifying blocksizes that will dividing data on the various cores and suggest a methodology that explore the memory hierarchy available in modern machines.

1 Introduction

Despite the increase in processing power and storage capacity of computers in recent decades [10], there is a growing demand by scientists, engineers, economists among others researchers, which are looking for high performance computing. This demand is due to a variety of complex problems being studied and also the increasing amount of data to be analysed.

In modern system platforms, a growing number of multiprocessors [7] has become available and researchers have been spending significant efforts to extract high performance from such systems [9]. In recent studies, the memory access pattern is a crucial

*Supported by CNPq and partially supported by the Brazilian Oil Company (Petrobras)

aspect when designing a 3D domain problem, as in the case of the stencil computations on regular grid [12], which appears in many problems of different areas.

In general, the CPU legacy codes are directed executed on multicore machines (normally, only a recompilation is necessary), without being tuned to the peculiarities of these multicore architectures. In this case, important features, as the cache memory hierarchy that are shared between different cores, are ignored. Thereby, efforts are necessary to improve the utilisation of cache memory, in order to increase performance.

An effective approach to diminish the memory access cost by increasing data locality is the technique called blocksize calculation or Tiling [1, 16, 17, 3], where the loops are separated into smaller ranges so that data will remain in the cache while required. The difficulty lies on identifying the block value that will lead to the smallest execution time.

The main objective of this work is to address the fact that when executing stencil application on multicore machines, performance is gained if memory hierarchy is well explored. An extensive analysis on the performance of a typical strategy that identifies efficient blocksize or tiling to be used on stencil computations is carried out. Based on this study, a blocksize specification methodology is suggested and a detailed evaluation shows its benefits when executing stencil application on multicore machines. Through an extensive experimental evaluation, this work suggests a simple way for scientists to identify an efficient blocksize, shown to be very close to the optimal one.

2 3D Stencil Computations

Partial differential equation solvers are often implemented using iterative finite-difference techniques that sweep over a spatial grid, performing nearest neighbour computations called stencils. These computations are employed by a variety of scientific applications in heat diffusion, electromagnetism, fluid dynamics and seismic imaging. In a stencil operation, each point in a regular grid is updated with weighted contributions from a subset of its neighbours in both time and space [12]. As can be seen in Figure 1(a), a new value for the dark cell is obtained by the weighted sum of the values in all three neighbour cells in all three dimensions in both directions.

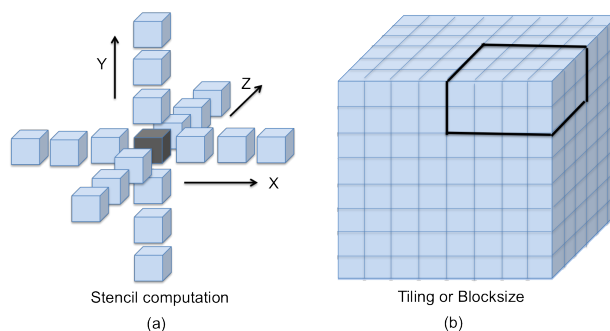


Figure 1: (a) Stencil computation of the dark point. (b) A blocksize for a 3D grid domain.

More specifically, in this work the behaviour of the stencil computation on the RTM application [16, 2] will be studied. The RTM is used to produce accurate imaging of new oil fields discovered in the Gulf of Mexico and in Brazil's southeast coast located in deep water, despite its high computational cost. The most time consuming part of the RTM algorithm is the computation of the 3D model, as indicated in line 5 of the RTM Algorithm 1, which is based on the difference finite method for PDE of the 10th order in space and 2nd order in time. This 3D method has a memory access pattern that refers to five points (cells) in each direction for each dimension to calculate the value of the actual point and actually, corresponds to 99% of the total execution time of the RTM application, as evaluated in [19].

In general, stencil calculations perform global sweeps through data structures that are typically much larger than the cache capacity, and also, data reuse is limited to number of neighbour points. Thus, optimisations are necessary to take full advantage of the memory hierarchy and to achieve high performance. The new multicore processors have some in-core optimisations to enhance performance, as for example, the Intel Streaming SIMD Extensions (SSE) allows data parallelism to execute the same operation on distinct elements in a data set [4]. However, the data parallelism will not be a significant help if the stencil computation underutilize cache lines. Data locality is the main target to achieve high performance in stencil computations.

On 3D stencil applications only one dimension has sequential data in memory which permits a fast execution, specially when vectorization is applied. On the other hand, the memory accesses considering the remaining directions are expensive. Therefore, some efforts are necessary to improve the data locality on such computations. One approach is to apply transformations to improve the cache memory utilisation. Loop splitting is an optimisation that breaks a loop into two or more loops, each one with fewer computations to reduce register utilisation. By splitting the stencil computation on independent x , y and z directions, the number of SIMD registers required to parallelise each loop is considerable smaller than the original one single whole loop [4]. Another effective approach is the technique called Tiling or Blocksize that will be explained in the next section.

Algorithm 1 :RTM ()

```

1  initialisation;
2  for each time step {
3   forall points: calculate energy;
4   forall points: calculate seismic;
5   forall points: calculate 3D model;
   }

```

3 Blocksize Technique for 3D Stencil Algorithms

The memory access pattern is a crucial aspect when designing a 3D domain problem, as in the case of the RTM kernel program [12]. An effective approach to diminish the memory access cost by increasing data locality is the technique called blocksize calculation or Tiling [1, 16, 17], where the loops are separated into smaller ranges so that data will remain in the cache while required. The difficulty lies in identifying the block size value that will lead to the smallest execution time. Figure 1(b) shows a block of elements to be traversed considering that its size has been calculated.

As a first step, this work shows a series of experiments that will portray the effect of the block size value on the application performance, focusing on stencil applications. For a better understanding of the performance, the Intel Vtune application profiler [11] is used.

3.1 Blocksize Profiler Analysis

Three versions of the sequential 3D model code for the problem size of $200 \times 200 \times 800$ was sampled in a node with two Intel Xeon E5410 2.33GHz Quad core processors with 12MB L2 Cache and 16GB of RAM memory per node. The only difference between the three versions analysed is the blocksize used. The first version, denoted as **No-Blocksize**, no blocksize technique was applied, while in a second version, called **Wrong-Blocksize**, inefficient blocksize was given ($159 \times 209 \times 175$) and finally, in the third version, denoted as **Efficient-Blocksize**, the application was executed with an efficient blocksize ($15 \times 15 \times 143$).

For this analysis, we consider a sample period of 50 iterations instead of the original 448 iterations in the remaining experiments evaluated in this paper. Table 1 presents the number of events that were collected for the three versions for a dedicated execution on only one unique core.

Table 1: Number of events collected by Vtune tool when executing one process of the application on one core

Events in millions ($\times 10^6$)	No-Blocksize	Wrong-Blocksize	Efficient-Blocksize
Clockticks	116,131	61,984	53,599
Retired instructions	56,845	63,445	65,561
L1 misses	1,275	1,013	1,026
Number of lines in L2	900	628	318
L2 misses	380	46	14
Number of cycles with stall	83,032	28,873	20,609
Number of bus cycles	16,522	8,846	7,762
Number of bus transactions	1,899	1,359	730

Efficient-Blocksize achieved the best performance, as justified by the smallest number of clockticks, since **Wrong-Blocksize** and **No-Blocksize** obtained values that

were 15.6% and 116.6% larger, respectively. Interestingly, Efficient-Blocksize produced more retired instructions than any other version, showing that the effectiveness of the code permitted the processor to retire more than one instruction per cycle, producing the smallest number of clockticks.

Concerning memory issues, Efficient-Blocksize also performed better than the other versions, specially when evaluating L2 cache related issues. Wrong-Blocksize and No-Blocksize produced 228.5% and 2,614.2%, respectively, more L2 cache misses than Efficient Blocksize. One can note that the Wrong-Blocksize and No-Blocksize allocated 97.4% and 183% more L2 cache lines than Efficient-Blocksize. Based on this event, the L2 cache miss rate derived for each version ($\frac{\text{Number of lines in L2}}{\text{Retired Instructions}}$) is 0.005, 0.010 and 0.016 for Efficient-Blocksize, Wrong-Blocksize and No-Blocksize, respectively. Actually, the cache miss rate for Efficient-Blocksize is an order of magnitude smaller than the other versions, what is reflected directly on the performance, showing the benefits of avoiding misses on higher memory levels.

Another event that portray memory access is the utilisation of the system memory bus (FSB), which connects the processor with RAM memory and can indicate performance bottlenecks. As can be seen in Table 1, the number of bus cycles is smaller for Efficient-Blocksize, meaning that a smaller number of accesses to external memory was necessary due to better data locality. The bus utilisation metric ($\frac{\text{Number of bus transactions} \times 2}{\text{Number of bus cycles}}$) for versions Efficient-Blocksize, Wrong-Blocksize and No-Blocksize are 0.19, 0.31 and 0.23, respectively.

Finally, the smallest number of clock cycles that stalls due to branch misprediction was for the Efficient-Blocksize version, while Wrong-Blocksize and No-Blocksize were 40% and 302% larger than it. The resource stall ratio ($\frac{\text{Number of cycles with stall}}{\text{clockticks}}$) confirms the better performance of version Efficient-Blocksize being only 38% and smaller than the other versions.

This same experiment was repeated for the three versions, however, instead on a dedicated node, the profiling of each version was executed together with another seven processes of the same version on the remaining cores of the node. This analysis is more representative in the sense that it reflects the actual memory utilisation of the execution of the RTM application (stencil computation) in multicore machines, when one process per core is executed. The results obtained are presented in Table 2.

Table 2: Vtune events executing on all 8 cores of a node

Events in millions ($\times 10^6$)	No-Blocksize	Wrong-Blocksize	Efficient-Blocksize
Clockticks	1,942,215	1,009,088	615,907
Retired instructions	405,280	505,356	468,642
L1 misses	10,229	8,309	7,488
Number of lines in L2	7,565	4,227	2,471
L2 misses	5,259	1,497	621
Number of cicles with stall	1,552,245	706,546	365,191
Number of bus cycles	253,593	124,845	88,002
Number of bus transactions	86,573	46,363	31,754

The results confirmed the advantages of the use of an efficient blocksize. For instance, the number of clock ticks produced by **Wrong-Blocksize** and **No-Blocksize** are, respectively, 63.8% and 215.3% larger than those of **Efficient-Blocksize**. Also, the number of L2 cache misses were more than twice smaller than **Wrong-Blocksize** and more than eight times smaller than **No-Blocksize**. When considering the clock cycles that stalls, the versions **Wrong-Blocksize** and **No-Blocksize** presented, respectively, 93,4% and 325% more than **Efficient-Blocksize**. Besides, the resource stall ratio for **Efficient-Blocksize** was the smallest amongst the three versions and the only one below 60%, which is considered the threshold for a efficient execution.

Finally, to evaluate the execution time of the application for the three cases, they were executed on one dedicated core of a node and also, on the eight cores of the node, one process per core, sharing the memory hierarchy. In both executions, each process computed 448 iterations for the $200 \times 200 \times 800$ problem size instance. The results can be seen in Table 3.

Table 3: Execution time of the three versions (in seconds)

Number of cores	No-Blocksize	Wrong-Blocksize	Efficient-Blocksize
1	390.0	279.1	234.3
8	1033.4	825.2	488.1

As was demonstrated by the VTune analysis, the performance of the version with efficient blocksize is clearly the best. When considering the execution in a dedicated node to the sole process the execution time of **Wrong-Blocksize** and **No-Blocksize** were 19.1% and 66.5% slower than the efficient blocksize one. More important, when considering the sharing of the resources of a node with other processes, the performance of **Efficient-Blocksize** were even more impressive, being the execution time of the **Wrong-Blocksize** and **No-Blocksize** 69% and 111.7% slower than it.

Note that, when executing with other processes sharing the available resources, all three versions should produce execution times close to the ones obtained by their respective execution on one core, since the problem size executed per process is the same. However, as it was analysed with the VTune tool, the sharing of the memory hierarchy has a deep impact in the execution, diminishing the performance of the application. Comparing the execution time on one core with the one on eight cores, an increase of 108%, for **Efficient-Blocksize** was detected. On the other hand, the two other versions were even worse, producing execution times on eight cores three times higher than on one core.

These two experiments definitely presented the advantages of an appropriated blocksize and, its benefits are even more striking if we consider larger problem sizes and an increase in the number of iterations. Thus, the next section presents an alternative approach to find efficient blocksizes in multicore machines.

3.2 A Framework for Profiling Technique

In order to identify the best value for the block size, a typical technique is dynamic profiling of the code under consideration, which is the division of the work among all the processing units available, during which each processing core calculates the execution time of a given number of iterations of the kernel with distinct block sizes. However, even for a small 3D problem size, testing all possible coordinates combinations is practically unfeasible. The approach as described in [19], specifies nC combinations of points x , y , and z (a block of elements to be transversed is then defined), which are first tested by executing a number nI of iterations of the program kernel with different block sizes (combinations) and chooses the block value associated with the smallest execution time.

The framework for profiling adopted in this work implements two distinct phases, the *selection* and *verification* phases, as described as follows:

Selection Phase: a fixed number of nC block values combinations are executed by the nP processes in accordance with a given distribution on the processing elements of the target system and evaluated in parallel. Each one of the nP processes executes only nI iterations of the RTM Kernel. The chosen block size is the one associated with a given criteria that optimises the execution time of the nI iterations of the kernel. This best execution time will be denoted as *MinTime*.

Verification Phase: each one of the nP processes executes nI iterations of the kernel altogether with the given best block value found during the selection phase. The execution time measured at this phase will be denoted *ActualTime*.

3.3 Approaches to identify the best blocksize

The two phase profiling framework was implemented on the so called Original Block (OB) methodology, where during the *selection phase*, each one of the nP processes executes $\frac{nC}{nP}$ blocksize combinations in any order. The blocksize with the minimal execution time is the chosen one.

Nevertheless, when the processes execute distinct blocksize combinations asynchronously during the selection phase, different amounts of cache memory might be allocated to each process, which can lead to a misleading evaluation. The main idea of the new approach is to force all cores of each node to evaluate the same block value combinations in similar order, so that the same amount of cache memory is allocated to each one of the processes of a given node (i.e. the cache memory is equally divided among the cores of a node).

This methodology is defined as the following. Let N be the total number of multicore nodes and let NC_i be the set of cores of node i . During the *selection phase*, the nC combinations are equally divided between the nodes and then, each one of the $|NC_i|$ cores of a each node evaluates $\frac{nC}{N}$ combinations in the same order, in three stages:

Stage 1: selection of the best blocksize of each core;

Stage 2: selection of the best blocksize of each node;

Stage 3: selection of the best blocksize among all nodes.

A visualisation of the execution of the three stages can be seen in Figure 2, where, in each core, a sequence of block values are evaluated and the best one is chosen.

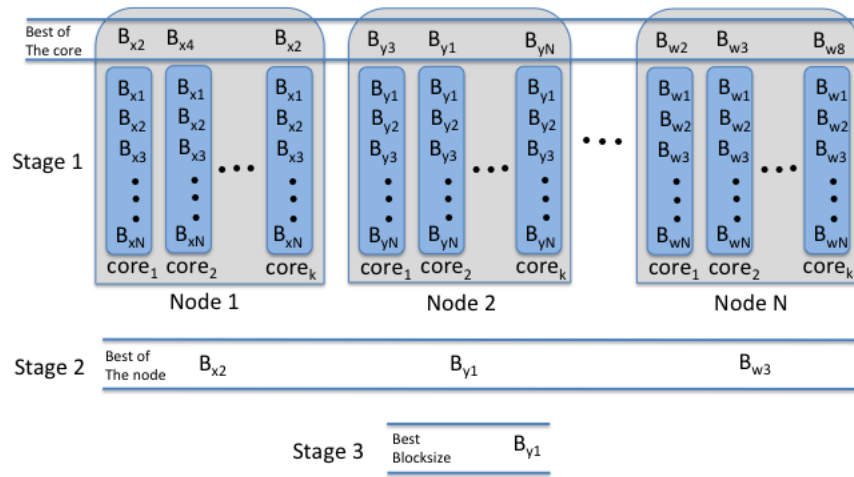


Figure 2: The three stages of the new approach for multicore machines

A natural approach is to choose the blocksize that minimises the execution time at each one of the three stages. For the first stage, this choice is the best one because the blocksize is chosen among completely distinct block values and the shared memory space is not considered. For the third stage, this choice is also the best one because the chosen one is evaluated considering distinct values on a non-shared memory space. This is not true for the second stage, during which although all the processes of a node (hopefully) evaluate the same block sizes in the same order, a minimisation function would not necessarily lead to the best value. This is due to the fact that there is no guarantee that the choice occurs on distinct values. Therefore, in this new algorithm, the first stage minimises its objective function, i.e. it chooses the blocksize with the smallest execution time since this is done sequentially by the process on its core. In the same manner, the third stage also minimises its objective function, since at this point, no cache influence occurs (data is allocated on the distributed memory). On the other

hand, during the second stage, three different approaches were evaluate: the choice of the block size that leads to the minimum, maximum and average executions time.

More formally, let $P_{k,i}$ be the process executing on core $c_{k,i} \in NC_i$ in node i . The time for nI iterations of the kernel to be executed by $P_{k,i}$ using block value b_k is given by $t(b_k, P_{k,i})$. In the first stage, each $P_{k,i}$ selects the block value $b_{k,i}^{min}$ such that $t(b_{k,i}^{min}, P_{k,i}) = \min_{\forall k} t(b_k, P_{k,i})$. Thus, as seen in Figure 2, at the end of this stage, each processor $P_{k,i}$ will have chosen a block value $b_{k,i}^{min}$, resulting in a total of $\sum_1^N NC_i$ blocksizes.

Then, in the second stage, the best block value amongst the cores in NC_i in node i considering each evaluated function is given by:

$$B_{NC_i}^{min} = \min_{P_{k,i} \in NC_i} \{t(b_{k,i}^{min}, P_{k,i})\} \quad (1)$$

$$B_{NC_i}^{max} = \max_{P_{k,i} \in NC_i} \{t(b_{k,i}^{min}, P_{k,i})\} \quad (2)$$

$$B_{NC_i}^{avg} = \min_{P_{k,i} \in NC_i} \left\{ \left| t(b_{k,i}^{min}, P_{k,i}) - \frac{\sum_{j=1}^i t(b_{k,i}^{min}, P_{k,i})}{i} \right| \right\} \quad (3)$$

At the end of the second stage, there will be N block values choses, one for each node i . Finally, in the third stage, the best block value b_{best} is such that

$$b_{best} = b_k \mid t(b_k, p) = \min_{\forall N_i} t(B_{N_i}^{target}, p_j)$$

is the one that provided the smallest execution time amongst all blocksize chosen for each node, where *target* is either *min*, *max* or *avg*, respectively. The mechanisms that calculate b_{best} based on $B_{N_i}^{min}$, $B_{N_i}^{max}$ and $B_{N_i}^{avg}$ are denoted as Min-Min-Min (*MMMB*), Min-Worst-Min Block (*MWMB*) and Min-Average-Min Block (*MAMB*), respectively.

3.4 Comparing the Original and Proposed Methodologies

Aiming to analyse the benefits and pitfalls of the strategies presented, a first series of experiments were carried out on a multicore cluster, called Oscar, composed of 40 BULL nodes, interconnected by Gigabit Ethernet, each node with two Intel Xeon E5430 2.66 GHz Quad core processors with 12MB L2 Cache and 16GB of RAM memory per node, running RHEL 5.3 and NFS.

An extensive analysis on three problem sizes: $200 \times 200 \times 800$, $300 \times 300 \times 800$ and $250 \times 250 \times 1500$, representing small, medium and large instances concerning the use of RAM memory, was reported in [19] and highlighted the fact that the execution times for the chosen blocksizes were not uniform, exhibiting a difference of 92% for problem size $300 \times 300 \times 800$ and of 96% for problem size $250 \times 250 \times 1500$, when comparing the smallest and largest execution times.

The difference between *MinTime* and *ActualTime* times as defined in Section 3.2, also called one's attention, since the same block values were used. These results showed that *OB* did not produce an adequate block value that maximises the cache utilisation on the target multicore systems. More specifically, let P_i and P_j be

two processes executing the selection phase of the algorithm in the same node N_k with two cores that share the cache memory. It is probable that P_i and P_j will execute with different blocksize values, such that distinct amounts of memory, for instance m_i and m_j , will be necessary. The size of cache shared by P_i and P_j reflects in the computational time of P_i and P_j . Let P_i be the process that identified the blocksize that produced the minimum time t_i . In the verification phase the processes will execute the code with the same block value, with an amount of memory m_i . However, in this execution, the actual execution time t'_i can be greater than t_i , because the amount of cache memory used by the two processes will be $2 \times m_i$ instead of $m_i + m_j$. This behaviour motivates the creation of the strategy proposed in the previous section, which produces a blocksize associated with a minimum time in the selection phase close to the actual execution time during the verification phase.

The proposed mechanisms were also executed on 128 cores of Oscar cluster for the three distinct problem sizes. The results provided were more homogeneous than *OB*, considering the 10 executions of each instance. Table 4 summarises these results (in seconds) where one can see the best, average and worst times considering the 10 executions associated with each algorithm and also the respective standard deviation (ST) for each problem size.

Table 4 shows that *MWMB* obtained the best results practically for all the instances analysed, losing only once (third line) for *MAMB*, but with a difference of less than 1.8%. Also, *MWMB* were significantly more efficient than *OB* and *MMMB*. Another important advantage of the *MWMB* and *MAMB* algorithms are the similarity of the block values calculated in all of the 10 executions. For all of the problem sizes, the standard deviation (ST) was very small, showing the accuracy and efficiency of the *MWMB* and *MAMB* algorithms. The main reason for such good results is that this technique provides a more fair division of the cache memory among the cores of a multicore node. A consequence of this efficiency when comparing the differences of *MinTime* and *ActualTime* times obtained by the selection and verification phases, respectively, being always less than 1% (Table 5, to be analysed later).

Therefore, from now on, the algorithm *MWMB* will be adopted as the basis of the study carried out in the remaining of this paper.

3.5 The quality of the selected blocksize

The next experiment exhaustively executes the RTM kernel for a different set of blocksize values in order to obtain the one with the smallest execution time. Comparing this blocksize value with the one produce by *MWMB* provides an opportunity to measure the quality of the proposed strategy.

When executing the RTM kernel for a $250 \times 250 \times 1500$ problem size instance per process, a total of $250 \times 250 \times 1500 \cong 94$ millions block combinations would be necessary to attain the best blocking value. In order to reduce the number of tests and thus carry out this experiment in a feasible time, the blocking values were tested at intervals of 16 points for i and j , and 32 points for k . This experiment was carried out on one eight cores Oscar machine.

Figures 3 and 4 presents the performance of the application according to the various blocksizes. Figure 3 shows that there is a large and conflicting variation on the

Table 4: Comparison of the four procedures

Results	problem size	OB	MMMB	MWMB	MAMB
best	$200 \times 200 \times 800$	914.3	700.3	621.0	678.0
	$300 \times 300 \times 800$	1279.4	1418.0	1278.2	1411.5
	$250 \times 250 \times 1500$	1926.5	2107.2	1891.1	1857.6
average	$200 \times 200 \times 800$	963.2	906.4	631.8	688.5
	$300 \times 300 \times 800$	1648.2	1537.0	1295.0	1443.8
	$250 \times 250 \times 1500$	3281.0	2439.7	1926.1	2043.7
worst	$200 \times 200 \times 800$	1145.4	981.0	655.3	698.0
	$300 \times 300 \times 800$	2467.5	2451.4	1313.2	1693.7
	$250 \times 250 \times 1500$	3674.6	3615.0	1958.3	2135.0
ST	$200 \times 200 \times 800$	68.2	107.7	10.2	6.4
	$300 \times 300 \times 800$	540.5	321.6	11.2	87.9
	$250 \times 250 \times 1500$	713.3	613.2	20.2	120.6

application performance as the values of k and j increase. While the performance of the application always diminishes as the value of j increases, there is an exponential decay as the value of k increases, but only for small values of k , more specifically until $k = 255$. After this point, a slight deterioration on the execution time is produced until the best value is reached, when a worsening can be seen.

Note that Figure 3 considers only $i = 15$, since the behaviour of the application for an increasing value of i is very similar. This can be seen in Figure 4, where j is set to 15 (one of the best values for this coordinate) while the values of i and k increases. One can see that the behaviour of the execution time as the value of k increases is the same as the one showed in the previous figure. It is also important to remark that there exists a variety of very efficient block sizes which are concentrated in the middle part of the curve, roughly between $k = 383$ and 1023 .

In order to analyse the quality of the block size produced by *MWMB* algorithm, a comparison of the execution times between the best block size found through the exhaustive search and the one found by *MWMB* algorithm is carried out. One of the best block sizes found by the exhaustive search was for $i = 183, j = 15, k = 511$. In the case of the *MWMB* algorithm for the same instance, the block size found was $47 \times 15 \times 511$.

As a matter of comparison, the RTM program was executed for a process workload of $250 \times 250 \times 1500$ with both block sizes values ($i = 183, j = 15, k = 511$ and $i = 47, j = 15, k = 511$) with an increasing number of processes. The results, shown in Figure 5, validate the effectiveness of algorithm *MWMB*, as the loss of performance was insignificant. In the worst case, the execution with the *MWMB* block size was only 2.4% longer than the one with best block size, while for executions with the largest number of processes, there was a loss of only 1.3%. Bear in mind that to identify the best block size via the exhaustive search, thousands of experiments were conducted during practically two months. Therefore, the quality of solution loss of *MWMB* is nothing comparable with the time spent to obtain it by the exhaustive search strategy.

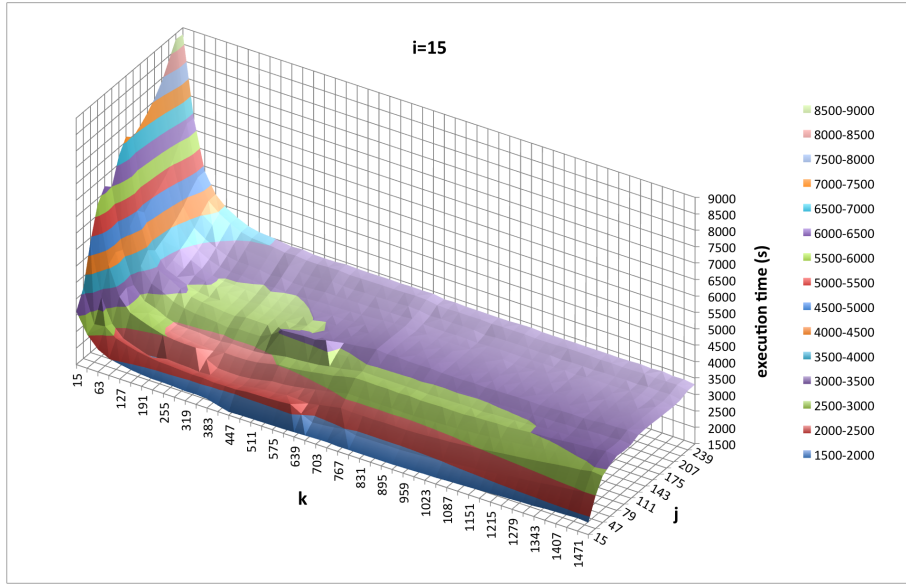


Figure 3: Execution times of the stencil application as the blocksize varies for $i = 15$

3.6 A metric to evaluate the quality of the blocksize

The blocksize produced by *MWMB* showed to be efficient, providing execution times very close to the one obtained through an exhaustive search. However, this evaluation and assurance of the quality was possible due to a large number of executions to identify the best blocking value.

Table 5 presents results for the instances $200 \times 200 \times 800$, $300 \times 300 \times 800$ and $250 \times 250 \times 1500$ considering *OB*, *MMMB*, *MWMB* and *MAMB*. The table shows one of the best blocksize produced by the corresponding methodology, the total execution time of the RTM application for the given blocksize, denoted as *Total*, the *MinTime* and *ActualTime* times, as already defined.

Based on a series of experiments carried out in this work, the comparison between *minimal* and *actual times* is proposed as a metric of the quality of the produced results. One aspect concluded is that when both *minimal* and *actual* times are close, the allocation of the shared memory during the *selection* phase reflects the allocation during the *verification* phase. Therefore, when the difference between the *MinTime* and *ActualTime* is negligible, the algorithm found a blocksize that leads to a faster execution when compared with the execution times of all the others blocksize. In other words, the closer are these two metrics, more efficient are the results.

As seen in Table 5, when *MinTime* and *ActualTime* are not near, the *Total* time is much higher than when both metric are close, since in this case, the new methodology succeeded in obtaining a blocksize in a specific condition that does reflect the actual memory hierarchy utilisation. For instance, the percentage difference of *MinTime* and *ActualTime* for the $250 \times 250 \times 1500$ problem size of the algorithms *OB*, *MMMB*,

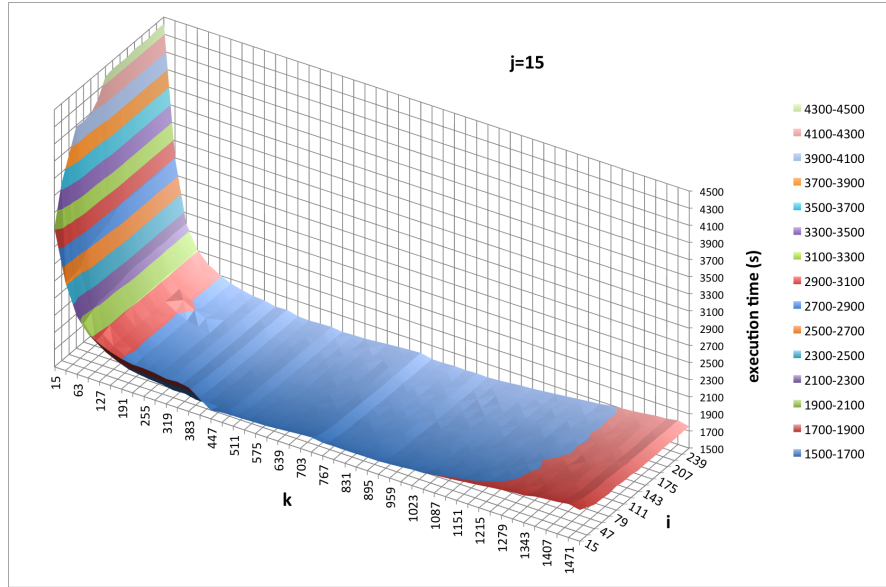


Figure 4: Execution times of the stencil application as the block sizes varies for $j = 15$

$MWMB$ and $MAMB$ were 126.8%, 28.1%, -0.2% and 23.2%, respectively, being the actual execution times produced their respective block sizes 3,646.3s, 2,146.2s, 1,949.0s and 2,121.3s.

Another aspect important to point out is that, the actual execution time (the verification phase execution time, $ActualTime$) of the RTM kernel having as input the block sizes identified by OB , $MMMB$ and $MAMB$ were 145.2%, 19.4% and 17.2% larger than the one associated with the block size identified by $MWMB$, respectively. Having in hands these block sizes and executing the original RTM parallel code leads to the execution time $Total$, which were 87%, 10.1% and 8.8% worse than the one executed with the block size produced by $MWMB$, respectively. Although, the $ActualTime$ is not the same as $Total$, since they depict the execution of different number of iterations of the RTM code, it can truly represent the performance of the four algorithms.

3.7 On the evaluation of the number of combinations analysed during the selection phase

This section investigates the quality of the block size obtained by $MWMB$ algorithm as the number nC of combinations tested during the *selection phase* increases. For doing so, the algorithm $MWMB$ is adapted to evaluate all the problem size domain according to the number of combinations to be tested. Being a 3D problem, the space domain is divided in the three dimensions and therefore, the combinations to be tested are chosen based on the number of divisions of the problem size. Let the size of each l dimension of the 3D problem be S_l . This S_l will be divided in P parts. Therefore, the

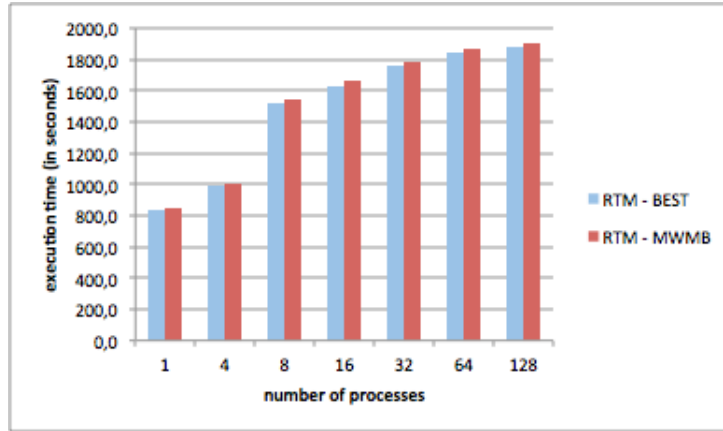


Figure 5: Comparison of the execution time of the RTM program with the best the *MWMB* blocksizes

Table 5: The impact of the comparison between Minimum and Actual times (*MinTime* and *ActualTime*) on the execution time of the original parallel application (*Total*)

problem size	algorithm	block value	<i>Total</i>	<i>MinTime</i>	<i>ActualTime</i>
200 × 200 × 800	OB	159 209 175	945.6	3.09	7.50
	MMMB	159 209 191	944.2	2.59	7.71
	MWMB	15 15 143	628.8	4.00	3.99
	MAMB	175 15 127	692.7	3.65	4.60
300 × 300 × 800	OB	15 15 127	1296.2	8.74	9.38
	MMMB	175 15 127	1452.5	6.35	10.82
	MWMB	15 15 159	1295.1	9.40	9.35
	MAMB	175 15 127	1414.5	8.77	10.85
250 × 250 × 1500	OB	159 259 607	3646.3	14.67	33.27
	MMMB	175 15 127	2146.2	12.65	16.20
	MWMB	47 15 495	1949.0	13.60	13.57
	MAMB	175 15 127	2121.3	12.91	15.90

values to be tested in the l -dimension are

$$b_l = \langle 1, \frac{S_l}{P-1} + 1, \frac{2S_l}{P-1} + 1, \frac{3S_l}{P-1} + 1, \dots, \frac{(P-1)S_l}{P-1} + 1 \rangle$$

Therefore, the total number of blocksize values tested are $nC = |b_i| \times |b_j| \times |b_k|$.

Table 6 shows the results of this experiment for three values of P (parts) of the problem domain: $P = 5, 10, 20$, resulting in three set of combinations ($nC = 125, 1,000$ and $8,000$). As an example, for the problem size $200 \times 200 \times 800$, the values tested for the i -dimension when $P = 5$ are the combination of : $b_i = \langle 1, 51, 101, 151, 200 \rangle$, $b_j = \langle 1, 51, 101, 151, 200 \rangle$ and $b_k = \langle 1, 201, 401, 601, 800 \rangle$, a total of $nC = 125$ combinations (note that the number of parts being evaluated are the same for all of the three dimensions, but this is not mandatory).

For each one of the three sets of combinations of each problem size instance, it was carried out a series of 10 executions in 8 nodes from Oscar of the RTM code with the produced best blocksize value, and a comparison with the execution time of the

selection phase under the *MWMB* procedure considering all the nC combinations of block values. The column **Total** represents the execution time of the RTM parallel code using the blocksize b_{MWMB} calculated by algorithm *MWMB*, while column $Total_{MWMB}$ shows the necessary time for *MWMB* to find b_{MWMB} , i.e. all the iterations necessary for *selection phase* considering all the nC combinations added to the *verification phase*.

As can be seen in Table 6, the time $Total_{MWMB}$ increases proportionally to the number of combinations, as expected. In the case of the $300 \times 300 \times 800$ problem size instance, while the total number of combinations tested increased from 125 to 1,000 and 8,000 (8 and 64 times more, respectively), the execution time of the selection phase $Total_{MWMB}$ increased 619% and 680%, respectively. On the other hand, the gain in performance as the number of combinations tested increased was quite modest. For instance, considering the average results for the $300 \times 300 \times 800$ problem size, while *MWMB* was executed practically 60 times longer evaluating 8,000 block-size combinations than the time spent to evaluate 125 combinations, the *Total* time spent to execute the original RTM parallel code with the best blocksize out of 8,000 combinations improved no more than 7%.

The performance for the other two problem sizes were similar, although for the $200 \times 200 \times 800$ problem size instance, the average *Total* time associated with the blocksize found when $nC = 8,000$ were slightly worse than the one associated with the blocksize for $nC = 1,000$. However, the smallest *Total* time amongst all the 10 executions for this instance for each number of combinations was 568.8 seconds, which was associated with $nC = 8,000$.

Figure 6(b) clearly shows the slight performance gain while $Total_{MWMB}$ (the execution time of the *selection phase*) drastically increases as the number of combinations nC grows (Figure 6(a)).

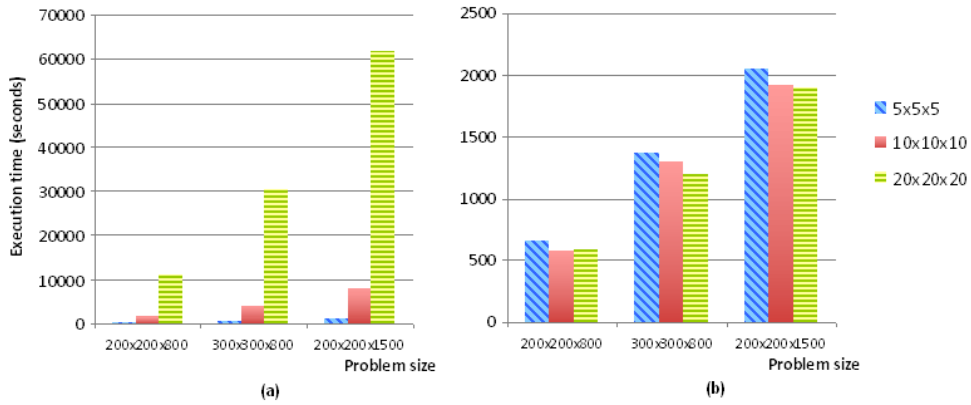


Figure 6: (a) Average execution time to find the blocksize by *MWMB*. (b) Total execution time produced by RTM using the blocksize calculated

When executing RTM application for a given instance for the first time, it is necessary to identify an efficient blocksize value, as already known. Suppose that the

Table 6: Total execution time of the RTM code (10 executions) using the blocksize b_{MWMB} produced by $MWMB$ and $Total_{MWMB}$ spent by the procedure to identify b_{MWMB} for nC combinations.

Size	Total of combinations tested					
	$P = 5 (nB = 125)$		$P = 10 (nB = 1,000)$		$P = 20 (nB = 8,000)$	
	$Total$	$Total_{MWMB}$	$Total$	$Total_{MWMB}$	$Total$	$Total_{MWMB}$
200	658.2	193.3	583.7	1422.2	568.8	10972.8
	660.8	192.6	593.4	1426.6	575.3	10970.0
	657.5	192.4	582.5	1427.8	655.1	10956.7
	656.2	191.2	577.3	1427.4	606.7	10973.4
	662.0	194.2	585.7	1443.5	578.2	10986.4
200 ×	656.0	192.3	592.2	1429.3	580.0	11122.1
	654.1	193.3	582.7	1428.4	585.0	11074.4
800	655.8	191.5	578.4	1432.5	574.9	11094.2
	653.7	195.3	588.4	1431.2	577.3	11064.9
	654.3	195.7	578.5	1435.8	599.0	11055.4
A	656.9	193.2	584.3	1430.5	590.0	11027.0
300	1370.1	541.7	1298.4	3908.4	1196.5	30407.2
	1359.8	542.1	1308.9	3899.1	1235.5	30869.8
	1366.6	543.1	1282.4	3899.3	1192.1	30316.1
300 ×	1369.4	541.6	1300.3	3901.1	1187.7	30329.6
	1379.2	540.1	1279.1	3901.1	1203.6	30407.5
800	1381.1	543.3	1308.9	3897.5	1238.1	30760.6
	1394.7	544.1	1267.1	3898.8	1185.5	30369.8
	1388.2	543.2	1311.6	3898.4	1211.8	30319.6
A	1364.3	540.9	1266.3	3897.3	1209.8	30265.6
	1377.6	544.0	1317.2	3888.8	1169.8	30236.0
A	1375.1	542.4	1294.0	3899.0	1203.0	30428.2
250	2033.2	1074.2	1906.5	7826.6	1898.8	61986.5
	2076.8	1082.4	1902.2	7863.9	1856.1	61327.9
250 ×	2075.6	1080.4	1926.9	7825.0	1885.7	61867.1
	2057.6	1059.9	1900.8	7850.9	1944.7	61348.8
1500	2060.4	1077.9	1934.8	7851.7	1944.3	61319.7
	2056.6	1079.8	1920.7	7813.4	1965.3	61655.8
	2066.7	1085.0	1935.6	7844.1	1947.9	61523.3
A	2024.7	1089.7	1912.4	7864.9	1847.7	61523.5
	2039.5	1074.4	1892.8	7815.7	1861.3	61732.1
	2031.0	1079.4	1922.6	7842.4	1859.7	61604.8
	2052.2	1078.3	1915.5	7839.9	1901.1	61588.9

application will be executed only once. In this case, the overall execution time would be $Total_{MWMB}(nC) + Total$, i.e. is the execution time taken by $MWMB$ to identify the best blocksize b_{nC} amongst nC combinations plus the execution time of RTM application using b_{nC} . Considering the best executions times (the smallest $Total$ for the 10 executions) for three distinct set of combinations ($nC = 125, 1,000$ and $8,000$) performed for the instance $250 \times 250 \times 1500$, $2,024.7s$, $1,892.8s$ and $1,847.7s$ and its respective $Total_{MWMB}(nC)$ $1,089.7s$, $7,815.7s$ and $61,523.5s$, it would be necessary for the RTM application using b_{125} to be executed 51 times more than RTM application using b_{1000} .

Thus, when choosing the number of combinations to be tested, the scientist should take into account the average execution time of the application and the number of times it will be executed. For applications that will run for a few hours, a small number of combinations is enough to provide a good blocksize and the algorithm will not be so intrusive. However, if the application is due to be running several times for many hours or days, a larger number of combinations should be tested.

4 Related Work

An investigation of the performance of evolving memory systems features, such as large on-chip caches, automatic prefetch, and the growing distance to main memory on 3D stencil computations was presented in [12]. The main observation is that improving cache reuse is no longer the dominant factor to consider in optimising these computations. In particular, the authors considered that streaming memory accesses are increasingly important because they engage software and hardware prefetch mechanisms that are essential to memory performance on modern microprocessors.

In [6] the impact of multicore architecture was analysed based on a case study with an Intel Dual-Core system. The main conclusion was that in these machines the intra-node communication has a significant impact and cache and memory contention can be a bottleneck. Thus, they state that the applications should be multicore aware to overcome these problems. The conclusions were made based on benchmarks. However, the study was poor in the sense that at most four nodes with two cores each were used.

In [8], a suite of optimisation mechanisms were evaluated considering a set of modern architectures. They developed an auto-tuning architecture aware environment similar to ATLAS and OSKI. The approach provided good performance across a variety of architectural configurations. The second component of an auto-tuner is the auto-tuning benchmark that searches the parameter space through a combination of explicit search for global maxima with heuristics for constraining the search space. At completion, the auto-tuner reports both peak performance and the optimal parameters.

In [15], a 3.5D blocking algorithm based on a 2.5D spatial blocking together with a temporal blocking on the input grid into an on-chip memory is proposed to increase the execution performance for Stencil Computations. The 2.5D spatial blocking blocks into two dimensions and then, outflows through the third dimension, in such a way that [15] advocates that the improvement on the on-chip memory utilization is due to the reduction on memory bandwidth usage. The temporal blocking executes multiple time-steps of the stencil computation, and thus data re-used. The performance of the algorithm is compared with other algorithms and it is faster for both CPU and GPU implementations, being almost linearly scalable. However, different from the work proposed here, the work does not infer how the dimensions of the blocking are calculated. Also, a good performance is only achieved if there is enough cache capacity to hold the blocked data.

In [5] the auto-tuning framework pOSKI for sparse linear algebra kernels on multicore systems is proposed as an extension of a previous work devised for cache-based superscalar uniprocessors. pOSKI applies a block compressed sparse row since it can achieve reasonable performance when proper register block size is selected. Both off-line and runtime auto-tuning mechanisms are conducted by pOSKI. The off-line auto-tuning considers a set of tunable parameters, collects benchmarking data, sparse matrix for a given architecture and compiler. Finally it selects the best implementation for each register block size. The authors advocate that although expensive, the off-line auto-tuning is effective since it is done once per architecture and compiler before running the application. The runtime auto-tuning is performed only after the matrix nonzero locations are known. Firstly, the sparse matrix is partitioned in sub-matrices compounded of consecutive row blocks with similar number of non-zeros per block,

each one executed by a thread. However, due to the use of different register block sizes, load unbalance can occur. Actually, a heuristic performs the register block size choice, which is only based on the number of non-zero elements. Also, the choice of an optimal number of cores is part of the auto-tuning problem. Currently, pOSKI just uses all available cores that are provided, since to identify the right number of cores is costly. Still, work has to be done on how to find a number of cores (not necessarily all the cores of a machine) in order to achieve good performance.

Versions of the Stencil kernel have been proposed and implemented not only on conventional CPU multicore processors, but also on FPGAs [14] and GPGPU [13, 18, 20]. General CPU systems are the most flexible, allowing a variety of optimizations and algorithmic manipulations. Furthermore, the majority of the RTM programs available are implemented in FORTRAN or C, using MPI or OpenMP, and are portable to these high performance platforms. Also, the CPU implementations allows to execute large domain problems with higher orders (and therefore, more points can be considered).

The work presented here is different from others, including the ones related to tiling techniques as presented in [1, 17], in the sense that it proposes an algorithm to optimise the use of memory hierarchy by 3D domain problems.

5 Concluding Remarks

Although the new CPU multicore machines are able to provide more computational power to the scientists, the performance of the 3D stencil applications depends on an efficient utilisation of the memory hierarchy of these machines. The tiling or blocking technique can be used to obtain an improvement of the data locality and thus a more efficient execution.

This work proposes a simple algorithm to produce an effective blocksize to be used in 3D stencil computations such as the RTM code or any problem where processes compete for shared cache space. More important, a new approach to utilise the multi-core machines are introduced in this algorithm and the results confirms the advantages of this technique. The benefits of this new algorithm were highlighted through a series of experiments and when compared with the best block obtained through exhaustive search for an specific problem size it was only 2% slower. Besides, experiments showed that a small number of combinations can produce very effective blocksizes and a simple way of evaluating the efficiency of the blocksize was presented.

References

- [1] J. Abella, A. Gonzalez, J. Llosa, and X. Vera. Near-optimal loop tiling by means of cache miss equations and genetic algorithms. In *Proceedings of the Inter. Conference on Parallel Processing*, pages 568–. IEEE Comp. Society, 2002.
- [2] M. Araya-Polo, F. Rubio, R. de la Cruz, M. Hanzich, J. Cela, and D. Scarpazza. 3D seismic imaging through reverse-time migration on homogeneous and heterogeneous multi-core processors. *Sci. Program.*, 17(1-2):185–198, 2009.

- [3] M. Baboulin, D. Becker, and J. Dongarra. A parallel tiled solver for dense symmetric indefinite systems on multicore architectures. In *Proceedings of IEEE International Parallel and Distributed Symposium (IPDPS 2012)*, 2012.
- [4] L. Borges and P. Thierry. 3D finite differences on multicore processors. <http://software.intel.com/en-us/articles/3d-finite-differences-on-multi-core-processors/>, 2011.
- [5] R. Byun, J. and Lin, K. Yelick, and J. Demmel. Autotuning sparse matrix-vector multiplication for multicore. Technical Report UCB/EECS-2012-215, EECS Department, University of California, Berkeley, Nov 2012.
- [6] L. Chai, Q. Gao, and D. K. Panda. Understanding the impact of multi-core architecture in cluster computing: A case study with intel dual-core system. In *Proceedings of the International Symposium on Cluster Computing and the Grid*, pages 471–478, DC, USA, 2007. IEEE Computer Society.
- [7] R. G. Clapp, H. Fu, and O Lindtjorn. Selecting the right hardware for reverse time migration. *The Leading Edge*, 29(1):48–58, 2010.
- [8] K. Datta, M. Murphy, V. Volkov, S. Williams, J. Carter, L. Oliker, D. Patterson, J. Shalf, and K. Yelick. Stencil computation optimization and auto-tuning on state-of-the-art multicore architectures. In *Proceedings of the 2008 ACM/IEEE conference on Supercomputing, SC '08*, pages 4:1–4:12. IEEE Press, 2008.
- [9] J. Dongarra, M. Faverge, H. Ltaief, and P. Luszczek. High performance matrix inversion based on LU factorization for multicore architectures. In *Proceedings of the 2011 ACM International Workshop on Many task Computing on Grids and Supercomputers (MTAGS)*, pages 33–42, 2011.
- [10] Jim Gray. What next? a dozen information-technology research goals. *Communications of the ACM*, 50(1):41–57, 2003.
- [11] Intel VTune. <http://software.intel.com/en-us/articles/intel-vtune-amplifier-xe/>, Last access 20/06/2012.
- [12] S. Kamil, P. Husbands, L. Oliker, J. Shalf, and K. Yelick. Impact of modern memory subsystems on cache optimizations for stencil computations. In *Proceedings of the 2005 Workshop on Memory System Performance, MSP '05*, pages 36–43, NY, USA, 2005. ACM.
- [13] P. Micikevicius. 3D finite difference computation on GPUs using CUDA. In *Proceedings of 2nd Workshop on General Purpose Processing on Graphics Processing Units*, pages 79–84. ACM, 2009.
- [14] T. Nemeth, J. Stefani, W. Liu, R. Dimond, O. Pell, and R. Ergas. *An implementation of the acoustic wave equation on FPGAs*, chapter 579, pages 2874–2878. Society of Exploration Geophysicists, 2008.

- [15] A. Nguyen, N. Satish, J. Chhugani, C. Kim, and P. Dubey. 3.5-D blocking optimization for stencil computations on modern CPUs and GPUs. In *Proceedings of the 2010 ACM/IEEE International Conference for High Performance Computing, Networking, Storage and Analysis, SC '10*, pages 1–13, DC, USA, 2010. IEEE Computer Society.
- [16] F. Ortigosa, M. Araya-Polo, F. Rubio, M. Hanzich, R. de la Cruz, and J. M. Cela. Evaluation of 3D RTM on HPC platforms. *SEG Expanded Abstracts*, 27:2879–2883, 2008.
- [17] G. Rivera and C. Tseng. Tiling optimizations for 3D scientific computations. In *Proceedings of the 2000 ACM/IEEE Conference on Supercomputing (CDROM)*, Supercomputing'00, DC, USA, 2000. IEEE Computer Society.
- [18] A. Schafer and D. Fey. High performance stencil code algorithms for GPGPUs. *Procedia Computer Science*, 4(0):2027 – 2036, 2011.
- [19] A. C. Sena, A. P. Nascimento, C. Boeres, V. E. F. Rebello, and A. Bulcao. An approach to optimise the execution of an RTM algorithm in multicore machines. *7th IEEE International Conference on e-Science*, pages 403–410, 2011.
- [20] J. Tao, M. Blazewicz, and S. Brandt. Using GPUs to accelerate stencil-based computation kernels for the development of large scale scientific applications on heterogeneous systems. *SIGPLAN Notes*, 47(8):287–288, 2012.